

AD-A066 631

NORTH CAROLINA UNIV AT CHAPEL HILL WILLIAM R KENAN JR--ETC F/6 9/1
AN X-RAY PHOTOELECTRON SPECTROSCOPIC STUDY OF MULTILAYERS OF AN--ETC(U)
MAR 79 A B FISCHER, M S WRIGHTON, M UMANA N00014-76-C-0817

UNCLASSIFIED

TR-8

NL

OF
AD
A066631



END
DATE
FILMED
5-79

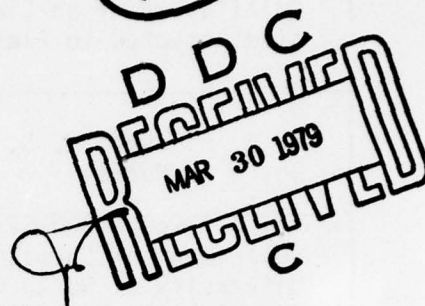
DDC

LEVEL II

OFFICE OF NAVAL RESEARCH

Contract N00014-76C-0817

Task No. NR 359-623



12 27 P1

14 TR-8

9 TECHNICAL REPORT, NO. 8

6 AN X-RAY PHOTOELECTRON SPECTROSCOPIC STUDY OF MULTILAYERS OF AN ELECTROACTIVE FERROCENE DERIVATIVE ATTACHED TO PLATINUM AND GOLD ELECTRODES.

15 N00014-76-C-0817^{by}

A. B. Fischer*, M. S. Wrighton*, M. Umana and Royce W. Murray

10 Alan B. Fischer, Mark S. Wrighton, M. Umana
Prepared for Publication in the
Journal of the American Chemical Society Royce W. Murray

11 5 Mar 79

University of North Carolina
Kenan Laboratories of Chemistry
Chapel Hill, North Carolina 27514

*Co-Authors, Massachusetts Institute of Technology, Cambridge, Massachusetts

March 1979

Reproduction in whole or in part is permitted for any purpose of the United States Government.

*Approved for Public Release and Sale, Distribution unlimited.

498 860

AD A0 66631
DDC FILE COPY

REPORT DOCUMENTATION PAGE		READ INSTRUCTIONS BEFORE COMPLETING FORM
1. REPORT NUMBER Technical Report #8	2. GOVT ACCESSION NO.	3. RECIPIENT'S CATALOG NUMBER
4. TITLE (and Subtitle) An X-Ray Photoelectron Spectroscopic Study of Multilayers of an Electroactive Ferrocene Derivative Attached to Platinum and Gold Electrodes		5. TYPE OF REPORT & PERIOD COVERED
		6. PERFORMING ORG. REPORT NUMBER
7. AUTHOR(s) A. B. Fischer, M. S. Wrighton, M. Umana and Royce W. Murray		8. CONTRACT OR GRANT NUMBER(s) N00014-76C-0817
9. PERFORMING ORGANIZATION NAME AND ADDRESS Department of Chemistry University of North Carolina Chapel Hill, NC 27514		10. PROGRAM ELEMENT, PROJECT, TASK AREA & WORK UNIT NUMBERS NR 359-623
11. CONTROLLING OFFICE NAME AND ADDRESS Office of Naval Research Department of the Navy Arlington, Virginia 22217		12. REPORT DATE March 5, 1979
		13. NUMBER OF PAGES twenty-two
14. MONITORING AGENCY NAME & ADDRESS (if different from Controlling Office)		15. SECURITY CLASS. (of this report) Unclassified
		15a. DECLASSIFICATION/DOWNGRADING SCHEDULE
16. DISTRIBUTION STATEMENT (of this Report) Approved for Public Release, Distribution Unlimited		
17. DISTRIBUTION STATEMENT (of the abstract entered in Block 20, if different from Report)		
18. SUPPLEMENTARY NOTES Prepared for publication in the Journal of the American Chemical Society		
19. KEY WORDS (Continue on reverse side if necessary and identify by block number) Chemically modified electrode, surface chemistry, ferrocene, X-ray photoelectron spectroscopy		
20. ABSTRACT (Continue on reverse side if necessary and identify by block number) Pretreated (anodized) Pt and Au electrode surfaces derivatized with (1,1'-ferrocenediyl)dichlorosilane have been analyzed by X-ray photoelectron spectroscopy (XPES). The derivatized surfaces exhibit Fe $2p_{3/2}$ bands with binding energies consistent with ferrocene iron and with large companion satellite peaks. Using a layer model, relative Fe $2p_{3/2}$ and electrode substrate intensities (Au or Pt) can be correlated with ferrocene coverage measured by cyclic voltammetry. The results indicate that electrochemical charge transfer can occur through ferrocene/silane layers of thicknesses exceeding 100 Å. —> ANGSTROM		

An X-Ray Photoelectron Spectroscopic Study of Multilayers of an Electroactive
Ferrocene Derivative Attached to Platinum and Gold Electrodes

Alan B. Fischer and Mark S. Wrighton*
Department of Chemistry
Massachusetts Institute of Technology
Cambridge, Massachusetts 02139

and

M. Umaña and Royce W. Murray*
Kenan Laboratories of Chemistry
University of North Carolina
Chapel Hill, North Carolina 27514

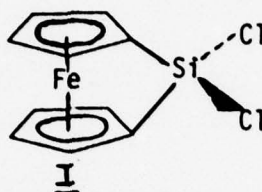
ACCESSION for	
NTIS	White Section <input checked="" type="checkbox"/>
DOC	Bull Section <input type="checkbox"/>
UNANNOUNCED	<input type="checkbox"/>
JUSTIFICATION	
BY	
DISTRIBUTION/AVAILABILITY CODES	
DI	SPECIAL
A	

79 03 26 01

Abstract

Pretreated (anodized) Pt and Au electrode surfaces derivatized with (1,1'-ferrocenediyl)dichlorosilane have been analyzed by X-ray photoelectron spectroscopy (XPES). The derivatized surfaces exhibit Fe $2p_{3/2}$ bands with binding energies consistent with ferrocene iron and with large companion satellite peaks. Using a layer model, relative Fe $2p_{3/2}$ and electrode substrate intensities (Au or Pt) can be correlated with ferrocene coverage measured by cyclic voltammetry. The results indicate that electrochemical charge transfer can occur through ferrocene/silane layers of thicknesses exceeding 100 \AA . XPES data indicate that the attached electroactive material contains less than the expected 1:1 ratio of Fe:Si, indicating some ferrocene degradation in the attachment procedure. These surface analyses accord well with elemental analyses of hydrolyzed material resulting from reaction of H_2O with (1,1'-ferrocenediyl)dichlorosilane which also shows less than a 1:1 Fe:Si ratio.

Our laboratories have recently described the attachment of organosilane reagents to the surfaces of oxidized platinum electrodes¹ and the electrochemistry of surfaces which result from reaction of (1,1'-ferrocenediyl)-dichlorosilane, I, with oxidized Pt and Au electrodes.^{2,3} Appropriately



pretreated Au and Pt electrodes derivatized with I exhibit cyclic voltametric waves at a potential which is within 100 mV of the formal potential for the ferricenium/ferrocene couple. These waves have properties expected⁴ of an electroactive moiety persistently attached to the electrode surface in both oxidized and reduced forms. The waves are quite persistent to repeated cyclical oxidation-reduction, and the charge under the waves corresponds to quite large and variable (from electrode to electrode) coverage ($\Gamma = 4\text{--}280 \times 10^{-10}$ mole/cm²) of the electrode surface by electroactive ferrocene. Coverages of these magnitudes require an interpretation involving a multilayer arrangement of ferrocene; e.g., it is probable that oligomerization of I occurs coincident with the electrode attachment reaction. The ability of such multilayered structures to undergo chemically reversible and, on certain electrodes, nearly electrochemically reversible ($\Delta E_{\text{peak}} \leq 10$ mv) reactions makes further study of these electrode materials of interest. In particular, the surface structural heterogeneity, implied by the variability in broadness and ΔE_{peak} of the cyclic voltammetric peaks, is a property of interest which can be studied by various surface sensitive physical methods. The present report describes the application of x-ray photoelectron spectroscopy (XPES) to a

series of oxidized Pt and Au electrodes which have been reacted with I. The data serve to confirm the presence of the ferrocene moiety and establish a rough, but positive, correlation between the quantity of ferrocene iron as detected electrochemically and by XPES.

EXPERIMENTAL

Preparation of electrodes and electrochemistry.

The ferrocene derivative I was that used in previous studies.^{2,3} Three sets of derivatized surfaces (two Pt and one Au) have been studied. Gold or platinum foil (0.01mm thick) was used to prepare an electrode such that both sides of $\sim 6 \times 40$ mm of surface was exposed. After cleaning the electrode in concentrated HNO_3 a 6×6 mm section (appropriate to mounting on the 0.25" XPES probe) was cut from the electrode as representative of a "clean" surface. The electrode was then pretreated according to previously^{2,3} established procedures and a second section (6×6 mm) of the foil strip, representative of the "pretreated surface", was removed from the electrode. The remaining portion of the foil electrode was derivatized with I as described previously. The electrode was then characterized by cyclic voltammetry in $0.1\text{M}[\text{n-Bu}_4\text{N}]\text{ClO}_4/\text{CH}_3\text{CN}$. A PAR 173/175 instrument with a Houston X-Y recorder was used. The reference electrode was an aqueous SCE. Three 6×6 mm sections were cut off the foil with a cyclic voltammogram before and after scission. In this manner the amount of electroactive material on each severed section can be determined. The three severed sections were washed thoroughly with CH_3CN and dried. The electrode itself

was stored in air at 298°K until after XPES analyses were performed as a control to insure prolonged attachment of the electroactive material. All samples for XPES analyses were shipped to Chapel Hill from Cambridge; two of the three derivatized sections were analyzed and one was returned to Cambridge for analysis by cyclic voltammetry to insure surface integrity during the transit. All control samples of derivatized surfaces exhibited essentially the same cyclic voltammetric behavior (peak positions, width, and integrated area) before and after the round trip to Chapel Hill. In some cases the time period involved exceeded eight weeks.

Hydrolysis of I.

XPES of the solid obtained from reaction of I with H_2O represents a useful comparison for XPES of surfaces derivatized with I. Hydrolysis was effected either by exposing a 2 ml isooctane solution of ~50 mg of I to atmospheric moisture and shaking for 24 h at 298°K or by injecting 0.5 ml liquid H_2O into a 2 ml isooctane solution of ~50 mg of I and shaking for 3 h at 298°K. The solid material was collected by filtration and washed with isooctane and H_2O . The solid was then dried under vacuum. Three such sets of samples were prepared; one set was analyzed by XPES and two sets were analyzed by elemental analysis by Galbraith giving $Fe/Si = 0.34$ (av); $C/Fe = 26$ (av).

X-Ray photoelectron spectroscopy.

XPES spectra were obtained on a DuPont Model 650B Electron Spectrometer⁵ equipped with a microprocessor system⁶ which controls pre-programmed spectral acquisition and tape storage. A TV screen operator-controlled cursor allows for baseline specification and automatic calculation of band (area) intensities. While smoothing capabilities exist, spectra presented here have not been smoothed. To minimize charging effects, electrodes were mounted on the spectrometer probe using conducting Ag paint. Standard compounds were run as powders on sticky tape with binding energies referenced to C 1s as 285.0 e.v.

RESULTS AND DISCUSSION

Electrochemical properties of the Pt and Au electrodes derivatized with I were similar to those discussed earlier.^{2,3} Formal potentials, peak potential separations, and electroactive coverages are given in Table I. Both coverage and general appearance of the cyclic voltammograms, Figures 1 and 2, indicate that the trans-shipment arrangements were satisfactory to protect the chemically modified surfaces.

All electrodes were examined at high resolution in XPES for Fe $2p_{3/2}$, N 1s, O 1s, Si 2s, Pt and Au $4f_{5/2,7/2}$, C 1s and Cl 2p. Survey scans detected no extraneous peaks. The complete absence of Cl 2p demonstrates that the reactive Si-Cl functionalities of I react completely as expected from their hydrolytic instability. The N 1s background present on all derivatized electrodes was consistently 2-4 times lower than on unreacted electrodes, consistent with pre-empting of electrode adsorption sites for nitrogeneous contaminants. Binding energy and intensity data are given in Table I. Table II contains binding energy and intensity data for some substituted ferrocenes for comparison. Examination of Fe $2p_{3/2}$ binding energies in ferrocene standards reveals a modest sensitivity to substituent. The electrodes to which I had been attached all exhibited prominent Fe $2p_{3/2}$ spectra as illustrated in Figure 3, curves 1-3. On five of the six electrodes examined, a Fe $2p_{3/2}$ peak was clearly visible at 707.9 ± 0.1 eV. On two of the electrodes (A and B) this peak had the same shape as ferrocenes such as 1,1'-ferrocenedicarboxylic acid (Figure 3, curves 3, 4). The 707.9 e. v. binding energy corresponds quite well to that observed for ferrocene in polymerized samples of I, Table II, which in turn lies within a range of energies compatible with ferrocene iron. This result confirms the expectation of the electrochemical behavior, that a ferrocene iron moiety has been attached to the surface of the Pt and Au electrodes.

A diffuse Fe $2p_{3/2}$ satellite band at 3 - 3.3 e.v. higher apparent binding energy than the main peak appears, erratically (Figure 3, curves 1-3) in the spectra of the surface attached ferrocenes. Electrode D showed mostly this satellite; the 707.9 e.v. band was barely visible. The satellite amplitude exhibits no particular pattern with coverage, etc. The cyclic voltammetric behavior of these multilayer ferrocene electrodes suggests,² however, that the chemical environment of the attached ferrocene can vary both within the polymer structure for a given electrode and from electrode to electrode. The satellite was also distinct in one of the polymerized samples of I (curve 6).

An extensive literature⁷ exists on energy loss satellites for transition metals including those of Fe $2p_{3/2}$ spectra. Energy loss satellites of Fe $2p_{3/2}$ vary in intensity and spacing from the main peak, according to the ligand in Fe complexes. The satellite is typically separated from the main peak by 4-5 e.v. Fe $2p_{3/2}$ energy loss effects normally, however, lead to satellites of considerably lower intensity than many of our spectral observations (e.g., curves 1,2,6 of Figure 3). While the observed satellites might reveal uncommonly efficient energy loss processes, and vary as a result of the structural variations within the multilayers as suggested by the electrochemistry, we think a chemical state interpretation of the satellites is more plausible.

XPES of a model ferricenium sample (Table II) shows a moderately broad $2p_{3/2}$ band at 709.5 e.v. On the other hand a mixed valence Fe(II), Fe(III) biferrocene spectrum⁸ exhibits a sharp 707.7 band (Fe(II)) plus an equal intensity but quite diffuse 711.1 e.v. band (Fe(III)). The latter has the same appearance as the 711 e.v. band in Figure 6. Additionally, ferrocene derivatives attached to carbon surfaces by three other completely different chemistries^{9a,b} also exhibit a broad 711 e.v. band, as well as the usual 708 e.v. ferrocene peak. In one case, we have shown that preliminary

reductive treatment substantially eliminates the 711 e.v. band. Finally, binding I to a high surface area, transparent substrate^{9c} reveals a blue-green (ferricenium) coloration of many specimens. These evidences lead us to interpret the broad 711 e.v. Fe 2p_{3/2} as a ferricenium state; e.g., the electrode preparation leaves a substantial fraction of the ferrocene sites in an oxidized state.

An alternate interpretation invoking differential charging of different ferrocene multilayer regions in the XPES experiment can be ruled out since the Si 2s and O 1s spectra exhibit no analogous satellites.

The efficiency of photoelectron production from ferrocene and ferricenium sites on electrodes coated with I should be the same. We have accordingly integrated the entire area of satellite plus main peak in the electrode bands as illustrated in Figure 3. This Fe 2p_{3/2} intensity is given relative to the substrate electrode metal (Pt or Au) in Table I. The ratio of intensities of iron and substrate electrode varies systematically with electrochemically measured coverage, an important result to which we will return.

The O 1s XPES on the ferrocene-multilayer electrodes was a single somewhat broad band whose intensity relative to that of electrode substrate is given in Table I. The binding energy of this band, 532.4 e.v., is entirely consistent with silicon-bound oxygen¹⁰ in accord with expectations of the mode of binding and polymerization of I on the electrodes.

XPES of oxidized but otherwise untreated Pt electrodes exhibits, Figure 4 (curve 4), a 4f doublet asymmetrically tailing on the high binding energy side as typical of Pt with a thin oxide layer.¹¹ In comparison, the "oxide" character of the Pt spectrum exhibited by the ferrocene multilayer electrode, Figure 4, curve 6, partially disappears upon reaction of the Pt surface with I. A similar and more dramatic effect is observed for the Au electrodes. Figure 4, curve 1, shows the Au 4f spectrum of the oxidized Au electrode; the spectrum is similar to that previously observed¹² on a similarly oxidized Au electrode. The measured 86.2 e.v. Au 4f_{7/2} binding energy agrees with that (85.9 e.v.) observed earlier and attributed to a layer of Au₂O₃ phase oxide. The oxide thickness is estimated very approximately

at 15 Å. Interestingly, upon reaction of the oxidized Au electrode with I, these prominent oxide phase bands disappear, leaving a Au 4f spectrum (curve 3) of very nearly the same shape as that of an otherwise untreated Au electrode (curve 2). The oxide is clearly removed in the silanization reaction medium. Apparently, the population of surface Au and Pt atoms involved in -M-O-Si-bonding is insufficiently large to be perceptible in the spectrum.

All electrodes exhibit a single, broad Si 2s band whose appearance was similar from electrode to electrode (Figure 3). Intensities relative to Fe 2p_{3/2} given in Table I are also similar from electrode to electrode. Conversion of intensities to a stoichiometric Fe/Si atom ratio for the attached ferrocene layer involves relative XPES elemental sensitivities as established either experimentally with standard compounds or with theory. The latter involves the ratio $\sigma_{\text{Fe}} \lambda_{\text{Fe,sil}} / \sigma_{\text{Si}} \lambda_{\text{Si,sil}}$, where σ is the photoelectron cross-section¹³ and λ is the escape depth for the respective element's photoelectrons in the ferrocene-silane layer. Using a model by Penn¹⁴ which indicates that escape depths of photoelectrons depend on kinetic energy approximately as $\lambda \propto (\text{K.E.})^{0.75}$, the theoretical relative sensitivity $[\text{Fe } 2p_{3/2}]/[\text{Si } 2s]$ is calculated at 7.26. An experimental relative sensitivity $[\text{Fe } 2p_{3/2}]/[\text{Si } 2s] = 9.06$ calculated from the standard compound in Table II agrees reasonably well with the theoretical value.

Application of the 9.06 relative sensitivity ratio to the ferrocene electrode results yields an average atom stoichiometry of 0.26 Fe/Si. Although this result is approximate, its deviation from the ideal 1/1 ratio is sufficiently great to strongly suggest that the electrode surfaces are Fe-poor. Perhaps oligomerization leads to expulsion of some ferrocene moieties, or oligomerization becomes terminated (e.g., ultimate coverage for a particular experiment achieved) by formation of a Si-rich siloxane layer at the ferrocene-solution interface. It is possible that this characteristic of the ferrocene multilayer plays an important role in the electrochemical properties.

XPES of hydrolyzed samples of I qualitatively accord well with the XPES of electrode surfaces derivatized with I in that the I_{Fe}/I_{Si} ratios reflect lower than 1/1 Fe/Si ratios in the sample, Table II. The variation in the I_{Fe}/I_{Si} ratios for the hydrolysis products suggests some inhomogeneity in the samples. Elemental analyses of hydrolysis products shows Fe/Si ratios in the range of 0.33-0.36 for three different samples but the C/Fe and C/Si ratios show substantial variation reflecting complex hydrolysis processes. The main point is that deliberate reaction of I with H_2O or with the electrode surface results in Fe-deficient material and the electroactive materials attached to such surfaces can not be strictly viewed as simple oligomers of ferrocenes linked by -Si-O-Si- bonds.

One of the most interesting aspects of the data of Table I is the correlation between the electrochemically-measured coverage and the ratio of XPES intensities Fe/Pt and Fe/Au. For the purposes of the following discussion, Pt and Au are identified as a common electrode substrate element M; this is a reasonable assumption inasmuch as the kinetic energy of 4f photoelectrons from these two materials is nearly identical. If the bonded ferrocene multilayer is considered a homogeneous, smooth layer overcoat of thickness d , the intensity of electrode substrate M relative to that of an uncoated electrode of element M is given by eq.(1).

$$\frac{I_M}{I_M^0} = \exp[-d/\lambda_{M,sil}] \quad (1)$$

where $\lambda_{M,sil}$ is the escape depth of the photoelectrons of M through the ferrocene/silane overlayer. Another relationship which can be derived for this layer model involves the relative intensities of ferrocene iron and M, eq. (2).

$$\frac{I_{Fe} \sigma_M^n \lambda_{M,M}}{I_M \sigma_{Fe}^n \lambda_{Fe,sil}} = \exp[d/\lambda_{M,sil}] - \exp[d/\lambda_{M,sil} - d/\lambda_{Fe,sil}] \quad (2)$$

where n is atoms/cm³ and λ is escape depth for the indicated element through the indicated medium. The thickness of the ferrocene overlayer, d , is related to the molar (moles/cm²) coverage by ferrocene through the average molecular weight of the immobilized ferrocene derivative and its intensity, eq. (3), where Γ is

$$d = 10^8 (MW) \Gamma / D_{\text{sil}} \quad (3)$$

molar coverage and D_{sil} is the density of the ferrocene silane layer. We will for the present identify the actual molar coverage of iron with the electrochemically measured molar coverage.

Previous papers^{11a,12,15} have correlated electrochemical coverages with XPES intensity ratios, but the situation represented by eq. (2) is more complex than these early cases, since the overlayer and the substrate elements are different. This leads to escape depth and relative cross-section terms in eq. (2) absent from the earlier situations.

Eq. (2) was compared to the Fe/Pt and Fe/Au intensity data of Table I in the following manner. As an initial approximation, the extreme righthand term of eq. (2) was set equal to zero, and a plot made of $\ln[I_{\text{Fe}}/I_{\text{M}}]$ versus Γ ; the resulting plot was reasonably linear. The intercept, $-\ln[\sigma_{\text{M}} n_{\text{M}} \lambda_{\text{M,M}} / \sigma_{\text{Fe}} n_{\text{Fe}} \lambda_{\text{Fe,sil}}]$ was dissected using theoretical cross-sections for σ_{M} and σ_{Fe} ,¹² 14.3 Å for $\lambda_{\text{M,M}}$,¹³ and average $n_{\text{M}} = 6.3 \times 10^{22}$ atoms/cm³ for Pt and Au, and a calculated¹⁴ $\lambda_{\text{Fe,sil}} = 13.9$ Å, from which $n_{\text{Fe}} = 3.45 \times 10^{21}$ atoms/cm³. From this result, taking MW = 244 (C₁₀H₈SiO₂Fe) a density of the ferrocene silane layer $D_{\text{sil}} = 1.40$ grams/cm³ is calculated. Considering that the density of ferrocene itself is 1.49 grams/cm³, and that measured for hydrolyzed I is 1.61 grams/cm³, this result is reasonable. The derived density is next employed with the plot's slope to estimate $\lambda_{\text{M,sil}} = 37$ Å, from which the extreme righthand term of eq. (2) was next calculated as a correction factor (it proves to be nearly negligible, ranging from 0.28 at low Γ to nearly zero at high Γ) and eq. (2) replotted. Figure 5 shows that the variation

of relative XPES Fe/M intensities correlates quite well with electrochemically-determined coverage. Ferrocene silane thickness calculated from XPES data with eq. (2) and from electrochemical coverages using eq. (3) and $D_{sil} = 1.4$ are listed in Table I.

Using the estimate of $\lambda_{M,sil}^0 = 37 \text{ \AA}$, values of ferrocene-silane thickness d were also calculated from eq. (1) and are listed in Table I. Considering that the latter calculation contains the uncertainty of comparing intensities measured on two separate electrode specimens, the correspondence between two different XPES analyses of d , by eq. (1) and (2), is quite satisfactory. Furthermore, a theoretical calculation¹⁴ of the escape depth $\lambda_{M,sil}$ yields 26 \AA which considering the accumulation of approximations made is in respectable agreement with the experimental value 37 \AA .

Two interesting features emerge from this analysis of the experimental data. First, apparent dimensions of the attached ferrocene silane overlayer are quite large. According to the analysis of Table I, electrochemistry on the electrode with highest coverage corresponds to charge transfer through well over 100 \AA of ferrocene-silane. It should be expected in such a situation that the perquisites for charge transfer are stringent and require both facile counterion mobility and a reasonably open structure. The dependence of the electrochemical behavior on the counterion in a comparison of perchlorate and tetraphenylborate³, and the variability of electrochemical reversibility from preparation to preparation are consistent with this view.

Secondly, the correspondence of an electrochemically measured quantity of ferrocene with a XPES-measured quantity of iron, Figure 5, indicates that to at least a first approximation all of the iron present is ferrocene iron and that all of the ferrocene iron is electroactive in the electrochemical experiment. This assertion has, of course, limitations with respect to the accuracy of the data fit represented in Figure 5, plus the uncertainties associated

with its assumption that the ferrocene-silane film has a uniform thickness. XPES relations which assume simple forms of non-uniformity (such as metal-exposing pores), when compared to equations (1) and (2), show I_M/I_{M^0} and I_{Fe}/I_M to be decreasingly responsive to film thickness at larger pore areas and at larger thicknesses. Model calculations indicate that effects of pores of area 10% of the total (causing ca. 30% error in d) could be accommodated within the data scatter. More extreme porosity would appear to be ruled out.

Acknowledgement. Research at UNC was supported by the National Science Foundation and the Office of Naval Research and at M.I.T. by the United States Department of Energy, Office of Basic Energy Sciences. We also thank J. R. Lenhard for useful discussions and Professor W. F. Little for generous gifts of a variety of ferrocene derivatives.

References

1. J. R. Lenhard and R. W. Murray, J. Electroanal. Chem., **78**, 195 (1977).
2. M. S. Wrighton, R. G. Austin, Andrew B. Bocarsly, J. M. Bolts, O. Haas, K. D. Legg, L. Nadjo, and M. C. Palazzotto, J. Electroanal. Chem., **87**, 429 (1978).
3. M. S. Wrighton, M. C. Palazzotto, A. B. Bocarsly, J. M. Bolts, A. B. Fischer, and L. Nadjo, J. Am. Chem. Soc., **100**, 0000 (1978).
4. R. F. Lane and A. T. Hubbard, J. Phys. Chem., **77**, 1401 (1973).
5. P. R. Moses, L. M. Wier, and R. W. Murray, Anal. Chem., **47**, 1882 (1975).
6. W. S. Woodward, J. L. Hinderliter-Smith, E. S. Brandt, and C. N. Reilley, in preparation.
7. (a) S. Larsson, Chem. Phys. Lett., **40**, 362 (1976); (b) T. A. Carlson, J. C. Carver, L. J. Keathre, F. G. Santibanez, and G. A. Vernon, J. Electron. Spectrosc., **5**, 247 (1974); (c) B. Walbank, I. G. Ilain, and C. E. Johnson, J. Electron. Spectrosc., **5**, 259 (1974); (d) J. C. Carver, G. K. Schweitzer, and T. A. Carlson, J. Chem. Phys., **57**, 973 (1972); (e) T. A. Carlson, J. C. Carver, and G. A. Vernon, J. Chem. Phys., **62**, 932 (1975).
8. D. O. Cowans, J. Park, M. Barber, and P. Swift, Chem. Commun., 1444 (1971).
9. (a) D.F. Smith, K. Willman, K. Kuo and R.W. Murray, J. Electroanal. Chem., **95**, 217 (1979); (b) R. Nowak, F.A. Schultz, M. Umana, H. Abruna and R. W. Murray, ibid., **94**, 219 (1978); (c) R.H. Staley, J.B. Kinney, A.B. Fischer, and M.S. Wrighton, to be submitted.
10. P. R. Moses, L. M. Wier, J. C. Lennox, H. O. Finklea, J. R. Lenhard, and R. W. Murray, Anal. Chem., **50**, 576 (1978).
11. (a) J. S. Hammond and N. Winograd, J. Electroanal. Chem., **78**, 55 (1977); (b) K. S. Kim, N. Winograd, and R. E. Davis, J. Am. Chem. Soc., **93**, 6296 (1971).
12. T. Dickinson, A. F. Povey, and P. M. A. Sherwood, J. Chem. Soc. Far. Trans. I, **71**, 298 (1975).
13. J. H. Scofield, J. Electron. Spectrosc. Relat. Phenom., **8**, 129 (1976).
14. D. R. Penn, J. Electron. Spectrosc. Relat. Phenom., **9**, 29 (1976).
15. T. A. Carlson and G. E. McGuire, J. Electron. Spectrosc., **1**, 161 (1972/73).

Table I. Electroanalytical and XPS Characterization of Derivatized Pt and Au Surfaces.

Table 1. Electroanalytical and XPS Characterization of Derivatized Pt and Au Surfaces.																
Expt. No.	Electrode	E^0 , V vs. SCE	Electroanalytical Data ^a			XPS Binding Energy, eV ^b				I_{Fe}/I_M	XPS Intensities			Layer Thickness, Å		
			ΔE_{peak} , mV	Γ , mol/cm ² × 10 ⁹	Fe 2p _{3/2}	Si 2s ^d	0 1s	M 4f _{7/2}	I_{Fe}/I_{Si}		I_0/I_M	I_C/I_M	I_{M/M^+} ^e	$d(Eq. 1)$ ^f	$d(Eq. 2)$ ^f	$d(Eq. 3)$ ^f
1 - Pt	A	0.455	50	4.1	707.8	153.2	532.4	70.4	0.176	----	2.15	2.67	0.103	84	60	71
1 - Pt	B	0.450	40	2.7	708.2	153.9	532.7	70.9	0.136	----	2.02	2.76	0.093	88	51	47
2 - Pt	C	0.445	70	1.7	707.8	153.6	532.4	71.2	0.083	2.18	0.70	0.51	0.554	22	36	30
2 - Pt	D	0.450	60	2.3	---	153.4	532.3	71.2	0.101	2.44	0.78	0.73	0.410	33	41	40
3 - Au	E	0.455	60	9.5	707.9	153.5	532.4	84.0	1.597	2.35	10.75	9.10	0.036 ₅	122	141	166
3 - Au	F	0.455	40	5.8	707.8	153.9	532.4	84.2	0.774	2.49	4.75	3.92	0.0789	94	114	101
	Avg.: 0.452		53	---	707.9	153.6	532.4	----	-----	2.37	-----	-----	-----	----	----	----

^aAll electroanalytical data are from cyclic voltammetry at 0.1 V/sec in 0.1M [(n-Bu)₄N]ClO₄ in CH₃CN solvent. E^0 is the average of anodic and cathodic peak potential. ΔE peak is the separation of anodic and cathodic peak; ΔE peak diminishes at lower scan rates. Γ is coverage of electroactive material from integration of anodic peak.

^bCorrected to C 1s = 285.0 e.V.

^cValue given is for the main, sharp Fe 2p_{3/2} peak. See Figure 3 and text for energy loss satellite.

^dThe normally more useful Si 2p band is obscured by the Pt, Au baseline.

^e Γ is Pt for electrodes A-D, Au for electrodes E and F; $\sigma(Pt 4f_{5/2+7/2}) = 15.84$; $\sigma(Au 4f_{5/2+7/2}) = 17.47$.

^fSee text.

Table II. XPS of Ferrocene Standards.

Sample	Binding Energy, e.V. ^a				XPS Intensities ^b	
	Fe 2p _{3/2}	Si 2s	Si 2p		I _{Fe} /I _{Si}	I _{Si2s} /I _{Si2p}
[Fe(η^5 -C ₅ H ₄ SiMe ₃) ₂] ^c BF ₄	709.5	152.1	---		4.53	----
Fe(η^5 -C ₅ H ₅)(η^5 -C ₅ H ₄ COMe)	708.8	---	---		----	----
Fe(η^5 -C ₅ H ₄ COOH) ₂	708.6	---	---		----	----
Fe(η^5 -C ₅ H ₅)(η^5 -C ₅ H ₄ (p-NH ₂ C ₆ H ₅))	708.2	---	---		----	----
Hydrolyzed I-slow ^d	708.3	153.7	102.6		6.26, 5.15	0.87, 0.99
Hydrolyzed I-fast ^d	708.0	153.6	102.6		1.85, 3.64	1.18, 0.97
Fe(η^5 -C ₅ H ₅) ₂	707.5	---	---		----	----

^aRelative to C 1s as 285.0 eV.^bRatio of band areas.^cRepeated scanning of this sample showed no reductive beam damage. A diffuse satellite at ~714 e.V. was observed for this sample.^dI hydrolyzed by exposure of an isooctane solution of I to atmospheric moisture (slow), Curve 5, Figure 3, or by deliberate injection of H₂O into isooctane solution of I (fast), Curve 6, Figure 3; see Experimental.

Figure Captions

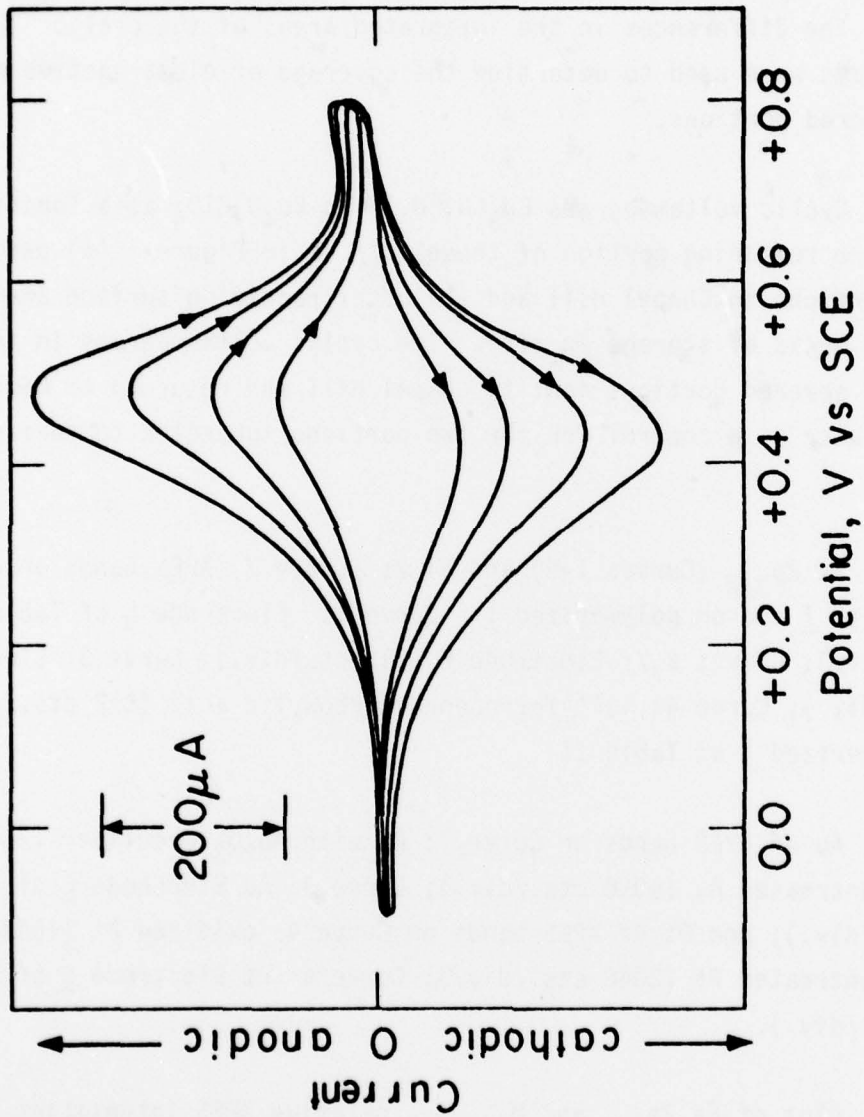
Figure 1. Cyclic voltammograms for Pt strip derivatized with I at 100 mV/sec in CH_3CN , 0.1M $[\text{n-Bu}_4\text{N}]\text{ClO}_4$. A portion of the electrode was severed after each scan and these three severed portions were shipped to Chapel Hill for surface analysis. The differences in the integrated areas of the cyclic voltammograms were used to determine the coverage of electroactive material on the severed portions.

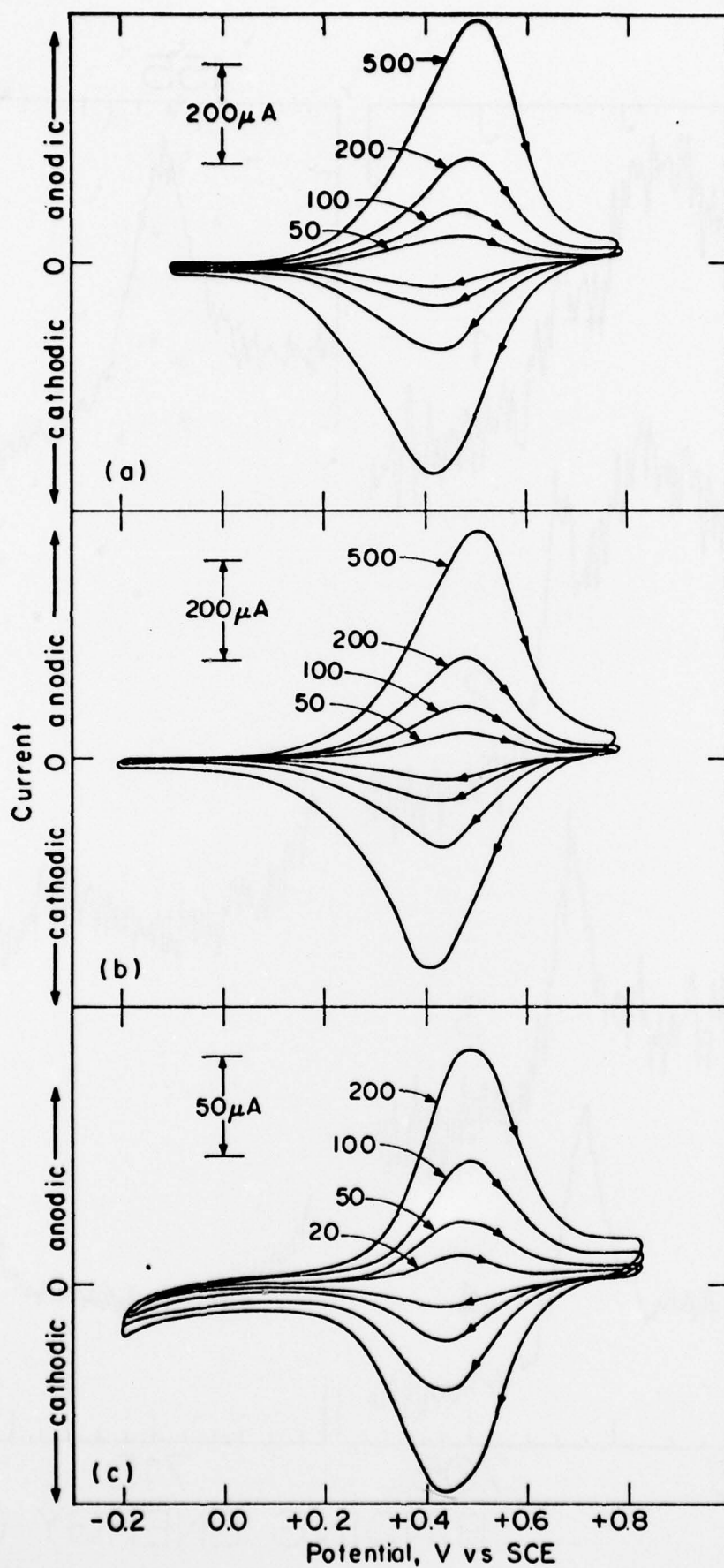
Figure 2. Cyclic voltammograms CH_3CN , 0.1M $[\text{n-Bu}_4\text{N}]\text{ClO}_4$ as a function of scan rate for the remaining portion of the electrode in Figure 1 (a) before sending severed portions to Chapel Hill and (b) after receiving surface analysis results (6 weeks of storage in air). The cyclic voltammograms in (c) are for one of the severed portions sent to Chapel Hill and returned to Cambridge ~6 weeks later as a control for the two portions subjected to surface analysis.

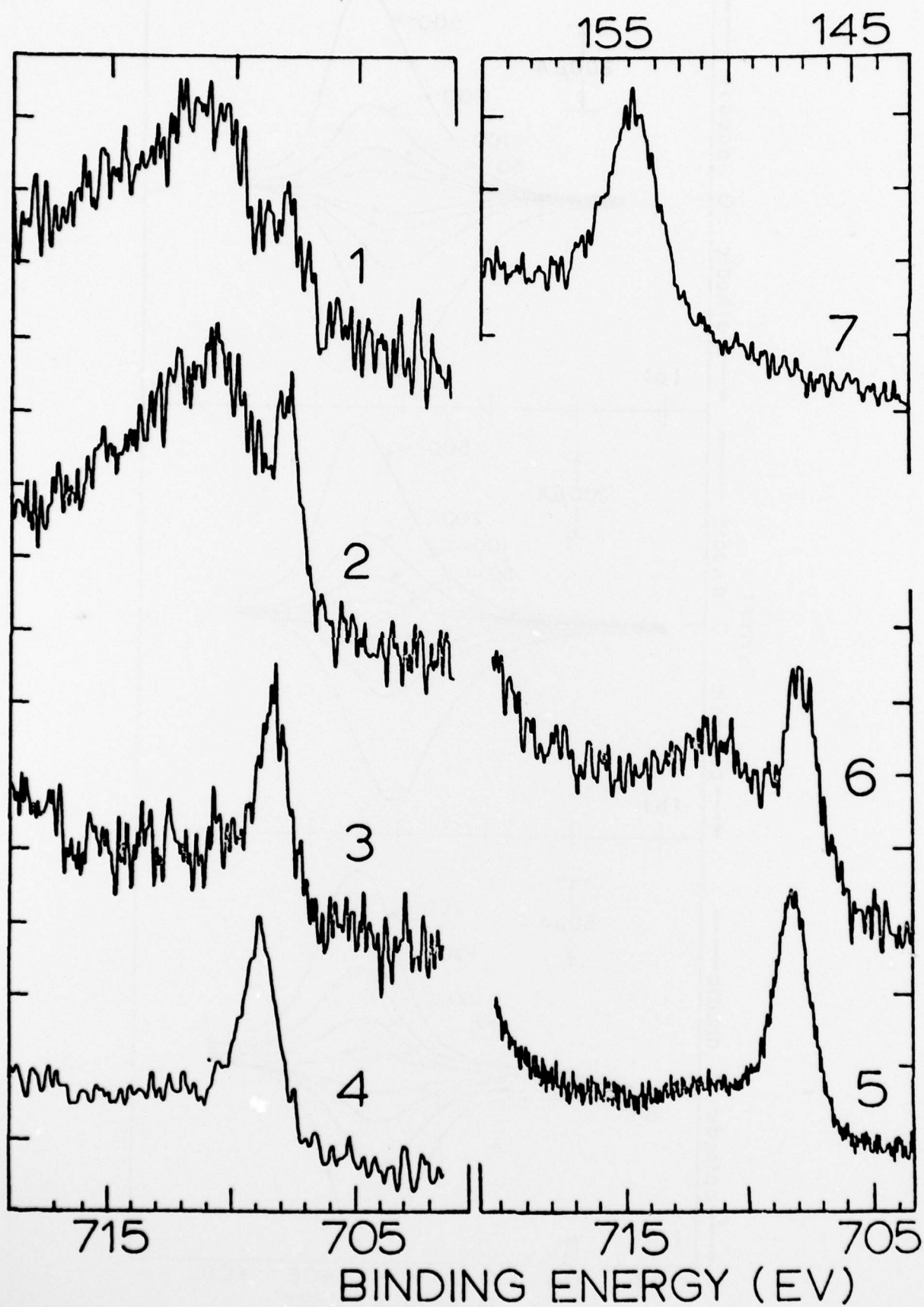
Figure 3. Fe $2p_{3/2}$ (Curves 1-6) and Si 2s (Curve 7) XPS bands on electrodes reacted with I and on polymerized I. Curve 1: Electrode C of Table I (256 counts/div.); Curves 2,7: Electrode F (512 cts/div.); Curve 3: Electrode B (512 cts/div.); Curve 4: 1,1'-ferrocenedicarboxylic acid (512 cts./div.); Curves 5,6: polymerized I of Table II.

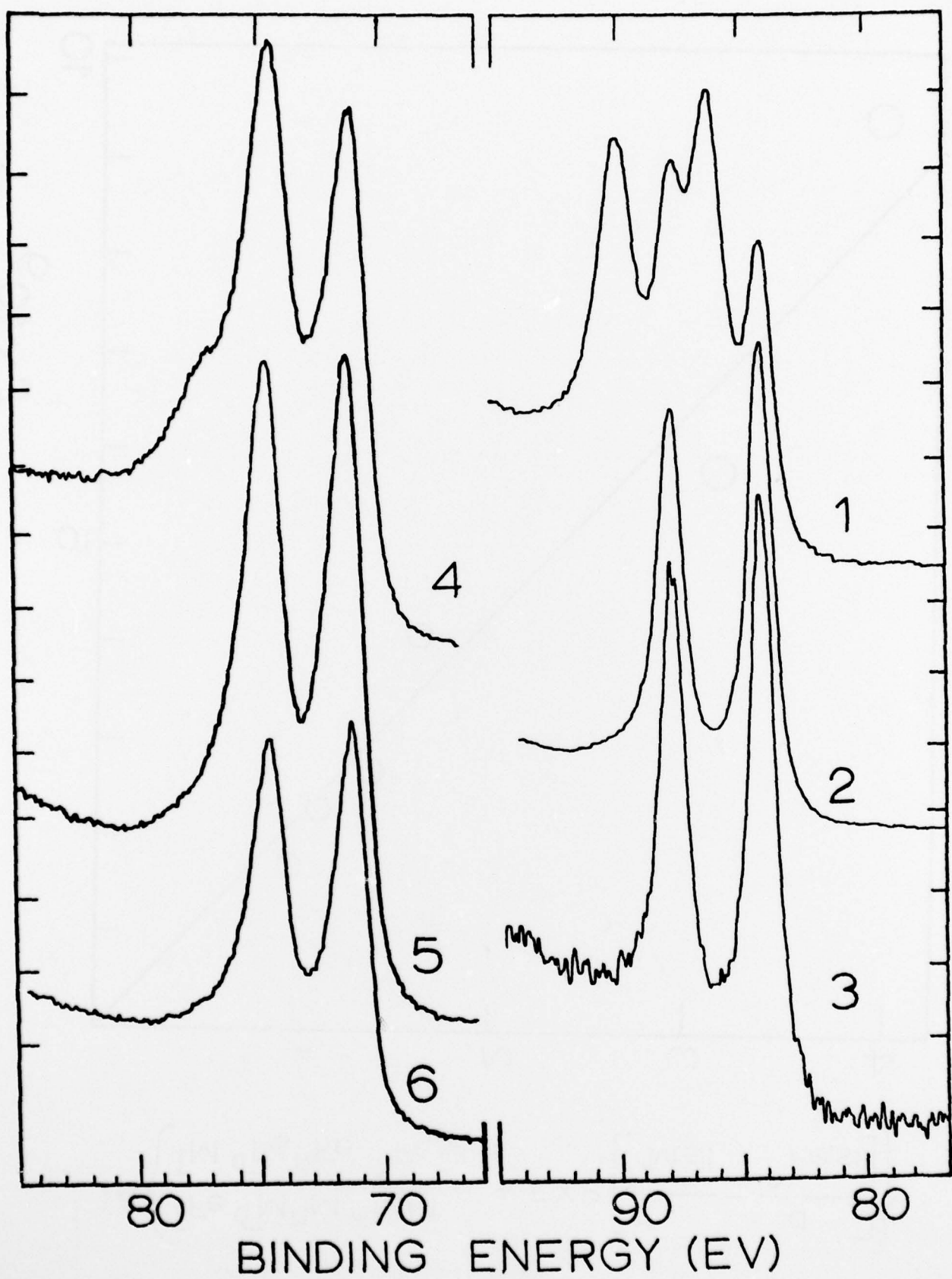
Figure 4. Au 4f XPS bands on Curve 1: Au with Au_2O_3 overlayer (2048 cts./div.); Curve 2: untreated Au (4096 cts./div.); Curve 3: Au Electrode F of Table I (256 cts./div.); and Pt 4f XPS bands on Curve 4: oxidized Pt (1024 cts./div.); Curve 5: untreated Pt (2048 cts./div.); Curve 6: Pt Electrode C of Table I (2048 cts./div.).

Figure 5. Plot of Fe $2p_{3/2}$ and $\text{M}_{5/2+7/2}$ relative XPS intensities in rearranged eq. (2) versus electrochemically measured coverage Γ , using parameters $\lambda_{\text{M,M}} = 14.3 \text{ \AA}$, $\lambda_{\text{Fe,sil}} = 13.9 \text{ \AA}$, $\lambda_{\text{M,sil}} = 37 \text{ \AA}$, $\eta_{\text{M}} = 6.3 \times 10^{22} \text{ atom/cm}^3$, and $\eta_{\text{Fe}} = 3.45 \times 10^{21} \text{ atoms/cm}^3$.

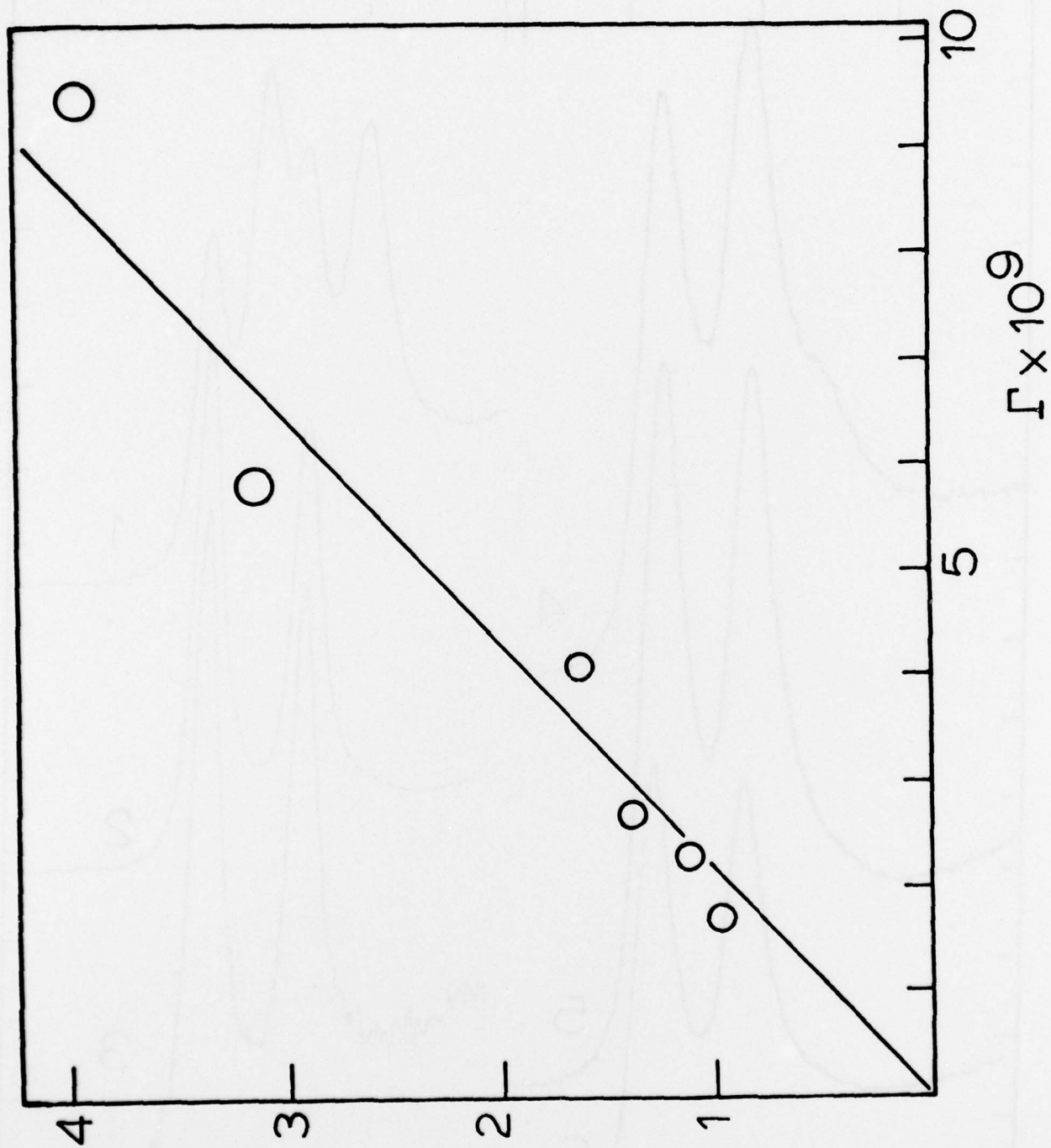








$$\ln \left\{ \frac{I_{Fe} \sigma_{MnM} \lambda_{M,M}}{I_M \sigma_{Fe}^n \lambda_{Fe,sil}} + \exp \left[\frac{\lambda_{M,sil}}{d} - \frac{\lambda_{Fe,sil}}{d} \right] \right\}$$



TECHNICAL REPORT DISTRIBUTION LIST, 359

	<u>No. Copies</u>		<u>No. Copies</u>
Dr. Paul Delahay New York University Department of Chemistry New York, New York 10003	1	Library P. R. Mallory and Company, Inc. Northwest Industrial Park Burlington, Massachusetts 01803	1
Dr. R. A. Osteryoung Colorado State University Department of Chemistry Fort Collins, Colorado 80521	1	Dr. P. J. Hendra University of Southampton Department of Chemistry Southampton SO9 5NH United Kingdom	1
Dr. E. Yeager Case Western Reserve University Department of Chemistry Cleveland, Ohio 41106	1	Dr. Sam Perone Purdue University Department of Chemistry West Lafayette, Indiana 47907	1
Dr. D. N. Bennion University of California Chemical Engineering Department Los Angeles, California 90024	1	Dr. Royce W. Murray University of North Carolina Department of Chemistry Chapel Hill, North Carolina 27514	1
Dr. P. A. Marcus California Institute of Technology Department of Chemistry Pasadena, California 91125	1	Naval Ocean Systems Center San Diego, California 92152 Attn: Technical Library	1
Dr. J. J. Auburn Bell Laboratories Murray Hill, New Jersey 07974	1	Dr. J. H. Ambrus The Electrochemistry Branch Materials Division, Research & Technology Department Naval Surface Weapons Center White Oak Laboratory Silver Spring, Maryland 20910	1
Dr. Adam Heller Bell Telephone Laboratories Murray Hill, New Jersey 07974	1	Dr. G. Goodman Globe-Union Incorporated 5757 North Green Bay Avenue Milwaukee, Wisconsin 53201	1
Dr. T. Katan Lockheed Missiles & Space Co, Inc. P.O. Box 504 Sunnyvale, California 94088	1	Dr. J. Boechler Electrochimica Corporation Attention: Technical Library 2485 Charleston Road Mountain View, California 94040	1
Dr. Joseph Singer, Code 302-1 NASA-Lewis 21000 Brookpark Road Cleveland, Ohio 44135	1	Dr. P. P. Schmidt Oakland University Department of Chemistry Rochester, Michigan 48063	1
Dr. B. Brummer EIC Incorporated Five Lee Street Cambridge, Massachusetts 02139	1		

	<u>No.</u> <u>Copies</u>		<u>No.</u> <u>Copies</u>
Office of Naval Research 800 North Quincy Street Arlington, Virginia 22217 Attn: Code 472	2	Defense Documentation Center Building 5, Cameron Station Alexandria, Virginia 22314	12
GNR Branch Office 536 S. Clark Street Chicago, Illinois 60605 Attn: Dr. George Sandoz	1	U.S. Army Research Office P.O. Box 1211 Research Triangle Park, N.C. 27709 Attn: CRD-AA-IP	1
ONR Branch Office 715 Broadway New York, New York 10003 Attn: Scientific Dept.	1	Naval Ocean Systems Center San Diego, California 92152 Attn: Mr. Joe McCartney	1
ONR Branch Office 1030 East Green Street Pasadena, California 91106 Attn: Dr. R. J. Marcus	1	Naval Weapons Center China Lake, California 93555 Attn: Dr. A. B. Amster Chemistry Division	1
GNR Area Office One Hallidie Plaza, Suite 601 San Francisco, California 94102 Attn: Dr. P. A. Miller	1	Naval Civil Engineering Laboratory Port Hueneme, California 93401 Attn: Dr. R. W. Drisko	1
ONR Branch Office Building 114, Section D 666 Summer Street Boston, Massachusetts 02210 Attn: Dr. L. H. Peebles	1	Professor K. E. Woehler Department of Physics & Chemistry Naval Postgraduate School Monterey, California 93940	1
Director, Naval Research Laboratory Washington, D.C. 20390 Attn: Code 6100	1	Dr. A. L. Slafkosky Scientific Advisor Commandant of the Marine Corps (Code RD-1) Washington, D.C. 20380	1
The Assistant Secretary of the Navy (R,E&S) Department of the Navy Room 4E736, Pentagon Washington, D.C. 20350	1	Office of Naval Research 800 N. Quincy Street Arlington, Virginia 22217 Attn: Dr. Richard S. Miller	1
Commander, Naval Air Systems Command Department of the Navy Washington, D.C. 20360 Attn: Code 310C (H. Rosenwasser)	1	Naval Ship Research and Development Center Annapolis, Maryland 21401 Attn: Dr. G. Bosmajian Applied Chemistry Division	1
		Naval Ocean Systems Center San Diego, California 91232 Attn: Dr. S. Yamamoto, Marine Sciences Division	1

TECHNICAL REPORT DISTRIBUTION LIST, 359

No.
Copies

Dr. H. Richtol
Chemistry Department
Rensselaer Polytechnic Institute
Troy, New York 12181

1

Dr. A. B. Ellis
Chemistry Department
University of Wisconsin
Madison, Wisconsin 53706

1

Dr. M. Wrighton
Chemistry Department
Massachusetts Institute of Technology
Cambridge, Massachusetts 02139

1

Larry E. Plew
Naval Weapons Support Center
Code 3073, Building 2906
Crane, Indiana 47522

1

S. Ruby
DOE (STOR)
600 E Street
Washington, D.C. 20545

1

Dr. Aaron Wold
Brown University
Department of Chemistry
Providence, Rhode Island 02192

1

Dr. R. C. Chudacek
McGraw-Edison Company
Edison Battery Division
Post Office Box 28
Bloomfield, New Jersey 07003

1

Dr. A. J. Bard
University of Texas
Department of Chemistry
Austin, Texas 78712

1

Dr. M. M. Nicholson
Electronics Research Center
Rockwell International
3370 Miraloma Avenue
Anaheim, California 92803

1

Dr. M. G. Sceats
University of Rochester
Department of Chemistry
Rochester, New York 14627

1